ACADEMIC PRESS

Available online at www.sciencedirect.com

SCIENCE DIRECT®

Journal of Sound and Vibration 265 (2003) 469–487

JOURNAL OF SOUND AND VIBRATION

www.elsevier.com/locate/jsvi

The dynamics of a cracked rotor with an active magnetic bearing

Changsheng Zhu[a,1], D.A. Robb[b,*], D.J. Ewins[b]

[a] *Department of Electrical Engineering, Zhejiang University, Hangzhou, Zhejiang 310027, People's Republic of China*
[b] *Department of Mechanical Engineering, Imperial College London, Centre of Vibration Engineering, London SW7 2BX, UK*

Received 25 June 2001; accepted 7 June 2002

Abstract

The dynamic characteristics of a cracked rotor with an active magnetic bearing (AMB) are theoretically analyzed in this paper. The effects of using optimal controller parameters on the dynamic characteristics of the cracked rotor and the effect of a crack on the stability of the active control system are discussed. It is shown that the dynamic characteristics of the cracked rotor with AMBs are clearly more complex than that of the traditional cracked rotor system. Adaptive control with AMBs may hide the fault characteristics of the cracked rotor, rather than helping to diagnose a crack; this will depend on the controller strategy used. It is very difficult to detect a crack in the rotor with an AMB support system when the vibration of the rotor system is fully controlled. Monitoring the super-harmonic components of $2\times$ and $3\times$ revolution in the sub-critical speed region can be used as an index to detect a crack in the rotor with an AMB system. If the effect of the crack is not taken into account at the design stage of the controller, then the rotor–AMB system will lose its stability in some cases when cracks appear.

1. Introduction

Active magnetic bearings (AMBs), which support shafts or rotors without any mechanical contact and lubrication, provide the possibility of designing high-speed rotating machinery. In addition, the AMB can actively control the vibration of rotor systems and improve their stability to meet the requirements of different operational states. The sensors and actuators in the AMB can also be used for on-line stimulation of the rotor for diagnosis. With further developments of

*Corresponding author. Tel.: +44-20-7594-7072; fax: +44-20-7584-1560.
E-mail addresses: cszhu@hotmail.com (C. Zhu), d.robb@ic.ac.uk (D.A. Robb), d.ewins@ic.ac.uk (D.J. Ewins).
[1] On leave from Department of Mechanical Engineering, Imperial College London, London, SW7 2BX, UK.

0022-460X/03/$ - see front matter
doi:10.1016/S0022-460X(03)00174-3

the complete AMB system, a smart machine technology (which integrates the AMB, fault diagnosis, prognosis and correction) can produce an optimal condition of the machine leading to higher performance and higher reliability for any state of the operation during the machine's life. This advanced technology is already a new research topic in rotating machinery.

The diagnosis of faults in an active rotor system with actuators is a key stage in the smart machine technology. Only if the faults are correctly diagnosed, can the system follow a correct adjustment procedure. In order to correctly diagnose faults, the basic dynamic behaviour of the active rotor system with faults must first be studied, since many differences exist in the fault characteristics between conventional rotor systems and active rotor systems. However, most research on the AMBs nowadays still focuses on structures of the AMB, the dynamics and modelling of the AMB–rotor system, control algorithms and some special problems related to AMBs. Few papers study the possibility of reliable fault diagnosis in the AMB–rotor system.

It is well known that cracks may appear in the rotating shaft due to the fatigue of the shaft material at some time during machine's life and these can result in calamitous accidents if undetected. There are a lot of papers dealing with the dynamics of the cracked rotor systems and the diagnosis of a crack in the rotating shafts as a comprehensive literature survey by Wauer [1] has shown. Either from the simplest model of the so-called de-Leval rotor or Jeffcott rotor [2–4] or from distributed parameter rotor systems with multi-bearing and multi-shaft [5–7], the basic conclusions are very similar. However, all work previously carried out on cracked rotors does not include the effect of the active control system. With the further development of active vibration control technology, especially after a series of successful applications of AMBs in high-speed rotating machinery, more and more advanced high-speed rotors will be built with controllable actuators. It is important to know the effect of the crack on the active control system and the effect of an active control system on the dynamic behaviour of the cracked rotor system. Recently, Zhu et al. [8] have analyzed, in general, the dynamics of a cracked rotor with an active feedback control system and shown that the dynamic characteristics of the active cracked rotor system are much more complex than that of the traditional cracked rotor system. There are many problems to be solved, for example, the effect of the crack on the control system stability, the diagnosis methods of the crack in the active rotor systems and the design of a stable controller, etc.

In the present paper, the dynamic characteristics of a cracked rotor supported on AMBs are studied; the effect of using optimal controller parameters on the dynamics of the active cracked rotor and the effects of crack on the control system are analyzed. A possible useful method for diagnosing the crack in the AMB–rotor system is proposed.

2. System model of the cracked rotor with AMB

2.1. Rotor model

The rotor system to be studied is a massless flexible shaft with a central disc, which is supported on two identical rigid bearings as shown in Fig. 1a. In order to simplify the analysis, an AMB is located at the disc position as a damper in order to control the vibration of the disc. There is a transversal crack close to the middle disc. The stiffness of the uncracked rotor system is symmetric and the damping at the middle disc due to the air resistance effect is viscous.

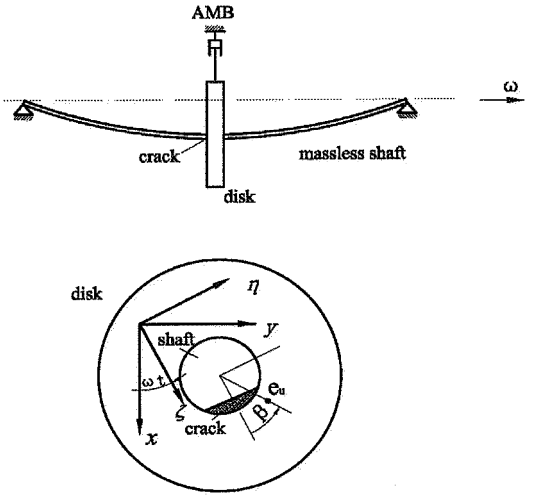

Fig. 1. The cracked rotor model with an AMB.

2.2. Equations of motion of the rotor system

The equations of motion of the rotor system in stationary Cartesian co-ordinates can be written as

$$\begin{bmatrix} m & 0 \\ 0 & m \end{bmatrix} \begin{Bmatrix} \ddot{x} \\ \ddot{y} \end{Bmatrix} + \begin{bmatrix} c & 0 \\ 0 & c \end{bmatrix} \begin{Bmatrix} \dot{x} \\ \dot{y} \end{Bmatrix} + \mathbf{K}(t) \begin{Bmatrix} x \\ y \end{Bmatrix} = \begin{Bmatrix} m\mathbf{g} \\ 0 \end{Bmatrix} + me_{\mu}\omega^2 \begin{Bmatrix} \cos(\omega t + \beta) \\ \sin(\omega t + \beta) \end{Bmatrix} + \begin{Bmatrix} F_x \\ F_y \end{Bmatrix}, \tag{1}$$

where x and y are the displacements of the disc in the stationary co-ordinate system, $\mathbf{K}(t)$ is the stiffness matrix of the cracked shaft in the disc position, m is the equivalent mass in the disc position, c is the viscous damping coefficient, e_{μ} is the imbalance eccentricity between the centre of the gravity and the geometric centre of the disc, β is the attitude angle of disc imbalance force vector with respect to the minimum stiffness direction of the crack shown in Fig. 1, $\mathbf{g}$ is the acceleration due to gravity, ω is the rotational speed of the rotor system, F_x and F_y are the feedback control forces produced by the AMB in the x and y directions, respectively.

2.3. Crack model

When a cracked rotor rotates slowly under the load of its own weight, the crack will open and close once per revolution. Therefore, the stiffness matrix of the shaft in the disc position $\mathbf{K}(t)$ is non-linear and periodical time varying during operation due to the effect of the crack. The periodic closing and opening of the crack is called "*breathing*" action [3,6]. Since an exact model of the "*breathing*" crack is quite complicated, the variation of stiffnesses of the cracked shaft in

the rotating co-ordinate system is often considered in the form

$$\begin{bmatrix} k_\zeta \\ k_\eta \end{bmatrix} = \begin{bmatrix} k_{m\zeta} + \Delta k_\zeta \cos \omega t \\ k_{m\eta} + \Delta k_\eta \cos \omega t \end{bmatrix}, \tag{2}$$

where k_ζ and k_η are the stiffnesses of the rotor in the minimum and maximum stiffness directions in the rotating co-ordinate system, ζ and η, shown in Fig. 1b. $k_{m\zeta}$ (or $k_{m\eta}$) and Δk_ζ (or Δk_η) are the average stiffness and the variations of stiffness of the cracked rotor in the ζ (or η) direction, respectively.

Transferring to the stationary co-ordinate system from the rotating co-ordinate system, one obtains the stiffness matrix of the cracked rotor in the stationary co-ordinate system as follows:

$$\mathbf{K}(t) = \begin{bmatrix} k_m + \Delta k \cos 2\omega t & \Delta k \sin 2\omega t \\ \Delta k \sin 2\omega t & k_m - \Delta k \cos 2\omega t \end{bmatrix}, \tag{3}$$

where

$$k_m = \tfrac{1}{4}\{[(k_0 + k_\eta) + (k_0 + k_\zeta)] + [(k_0 - k_\eta) + (k_0 - k_\zeta)] \cos \omega t\},$$
$$\Delta k = \tfrac{1}{4}\{[(k_0 + k_\eta) - (k_0 + k_\zeta)] + [(k_0 - k_\eta) - (k_0 - k_\zeta)] \cos \omega t\}.$$

2.4. AMB model

The relationships between the magnetic force and the applied currents in the coils can be found after neglecting magnetic saturation, hysteresis, magnetic flux leakage and eddy current loss. For the radial AMB with two opposite pairs of symmetrically electromagnetic poles, the linearizing magnetic forces of the radial AMB can be expressed as

$$\begin{Bmatrix} F_x \\ F_y \end{Bmatrix} = \begin{bmatrix} k_{sx} & 0 \\ 0 & k_{sy} \end{bmatrix} \begin{Bmatrix} x \\ y \end{Bmatrix} + \begin{bmatrix} k_{ix} & 0 \\ 0 & k_{iy} \end{bmatrix} \begin{Bmatrix} i_x \\ i_y \end{Bmatrix} = \mathbf{K}_S \begin{Bmatrix} x \\ y \end{Bmatrix} + \mathbf{G} \begin{Bmatrix} i_x \\ i_y \end{Bmatrix}, \tag{4}$$

where $\mathbf{K}_S$ and $\mathbf{G}$ are the displacement and the current stiffness matrices of the AMB, respectively, x and y are the displacements of the disc from the nominal air-gap, i_x and i_y are the control currents in the x- and y-electromagnets.

For the four pairs of symmetrically radial AMBs, the stiffness elements are

$$k_{sx} = \mu_0 A N^2 i_{0x}^2 \cos^2(\pi/8)/s^3, \quad k_{sy} = \mu_0 A N^2 i_{0y}^2 \cos^2(\pi/8)/s^3, \tag{5a}$$

$$k_{ix} = -\mu_0 A N^2 i_{0x} \cos(\pi/8)/s^2, \quad k_{iy} = -\mu_0 A N^2 i_{0y} \cos(\pi/8)/s^2, \tag{5b}$$

where s is the nominal air-gap, i_{0x} and i_{0y} are the bias currents in the x- and y-electromagnets, respectively, $\mu_0 = 4\pi \times 10^{-7}$ H/m is the air permeability, N is the number of the windings of the coil, A is the flux cross-sectional area of the air-gap.

2.5. Non-dimensional equations of motion of the rotor system

Substituting Eqs. (3) and (4) into Eq. (1), one obtains the general equations of motion of the cracked rotor with the AMB in the steady state case as follows:

$$\begin{bmatrix} m & 0 \\ 0 & m \end{bmatrix} \begin{Bmatrix} \ddot{x} \\ \ddot{y} \end{Bmatrix} + \begin{bmatrix} c & 0 \\ 0 & c \end{bmatrix} \begin{Bmatrix} \dot{x} \\ \dot{y} \end{Bmatrix} + \begin{bmatrix} k_m + \Delta k \cos 2\omega t - k_{sx} & \Delta k \sin 2\omega t \\ \Delta k \sin 2\omega t & k_m + \Delta k \cos 2\omega t - k_{sy} \end{bmatrix} \begin{Bmatrix} x \\ y \end{Bmatrix} = \begin{Bmatrix} m\mathbf{g} \\ 0 \end{Bmatrix} + me_\mu \omega^2 \begin{Bmatrix} \cos(\omega t + \beta) \\ \sin(\omega t + \beta) \end{Bmatrix} + \begin{bmatrix} k_{ix} & 0 \\ 0 & k_{iy} \end{bmatrix} \begin{Bmatrix} i_x \\ i_y \end{Bmatrix}. \tag{6}$$

Dividing both sides by $m\omega^2\delta_{st}$, one obtains the non-dimensional equations of motion of the cracked rotor system with the AMB as

$$\begin{bmatrix} 1 & 0 \\ 0 & 1 \end{bmatrix} \begin{Bmatrix} X'' \\ Y'' \end{Bmatrix} + \frac{1}{\Omega} \begin{bmatrix} 2\xi & 0 \\ 0 & 2\xi \end{bmatrix} \begin{Bmatrix} X' \\ Y' \end{Bmatrix} + \frac{\bar{\mathbf{K}}(\tau) - \bar{\mathbf{K}}_S}{\Omega^2} \begin{Bmatrix} X \\ Y \end{Bmatrix} = \frac{1}{\Omega^2} \begin{Bmatrix} 1 \\ 0 \end{Bmatrix} + U \begin{Bmatrix} \cos(\tau + \beta) \\ \sin(\tau + \beta) \end{Bmatrix} + \frac{\bar{\mathbf{G}}}{\Omega^2} \begin{Bmatrix} i_x \\ i_y \end{Bmatrix}, \tag{7}$$

where $X = x/\delta_{st}$, $Y = y/\delta_{st}$, $U = e_\mu/\delta_{st}$ is the rotor imbalance parameter, $\xi = c/2\,m\omega_{cr}$ is the viscous damping ratio, $\Omega = \omega/\omega_{cr}$ is the rotational speed ratio, δ_{st} is the corresponding deformation of the shaft due to the weight of the rotor, $\omega_{cr} = \sqrt{k_0/m}$ is the critical speed of the uncracked rotor, k_0 is the stiffness of the uncracked rotor, and $\tau = \omega t$ is non-dimensional time. The prime refers to differentiation with respect to τ.

$\bar{\mathbf{K}}(\tau)$ is the non-dimensional stiffness matrix of the cracked rotor and is given by

$$\bar{\mathbf{K}}(\tau) = \begin{bmatrix} \bar{k}_m + \Delta\bar{k}\cos 2\tau & \Delta\bar{k}\sin 2\tau \\ \Delta\bar{k}\sin 2\tau & \bar{k}_m - \Delta\hat{k}\cos 2\tau \end{bmatrix}, \tag{8}$$

where

$$\bar{k}_m = \tfrac{1}{4}\{[(1 + \bar{k}_\eta) + (1 + \bar{k}_\zeta)] + [(1 - \bar{k}_\eta) + (1 - \bar{k}_\zeta)]\cos\tau\},$$

$$\Delta\bar{k} = \tfrac{1}{4}\{[(1 + \bar{k}_\eta) - (1 + \bar{k}_\zeta)] + [(1 - \bar{k}_\eta) - (1 - \bar{k}_\zeta)]\cos\tau\}.$$

$\bar{k}_\eta$ and $\bar{k}_\zeta$ are the ratios of the stiffness of the cracked rotor in the η and ζ directions to the stiffness of the uncracked rotor k_0, respectively, and depend on the crack depth. In general, the variation of $\bar{k}_\eta$ with the crack depth is very small in comparison with the variation of $\bar{k}_\zeta$, so $\bar{k}_\eta$ is often considered unchanged with the crack depth, but any decrease of $\bar{k}_\zeta$ indicates an increase of the crack depth.

$\bar{\mathbf{K}}_S$ and $\bar{\mathbf{G}}$ are the non-dimensional additional displacement and current stiffness matrices of the AMB respectively and given by [10]

$$\bar{\mathbf{K}}_s = \frac{1}{k_0}\begin{bmatrix} k_{sx} & 0 \\ 0 & k_{sy} \end{bmatrix}, \quad \bar{\mathbf{G}} = \frac{1}{m\mathbf{g}}\begin{bmatrix} k_{ix} & 0 \\ 0 & k_{iy} \end{bmatrix}. \tag{9}$$

From Eq. (7), the state space equations of the cracked rotor with the AMB can be written as

$$\mathbf{q}' = \begin{bmatrix} \mathbf{0} & \mathbf{I} \\ -\underline{\mathbf{M}}^{-1}\underline{\mathbf{K}}(\tau) & -\underline{\mathbf{M}}^{-1}\underline{\mathbf{C}} \end{bmatrix}\mathbf{q} + \begin{bmatrix} \mathbf{0} \\ \underline{\mathbf{M}}^{-1}\underline{\mathbf{G}} \end{bmatrix}\mathbf{u} + \mathbf{f}_e = \mathbf{A}\mathbf{q} + \mathbf{B}\mathbf{u} + \mathbf{f}_e, \tag{10}$$

where $\underline{\mathbf{M}}_{2\times 2} = \mathbf{I}$ and $\underline{\mathbf{C}}_{2\times 2} = diag(2\xi/\Omega)$ are the mass and the damping matrices of the rotor system, respectively: $\underline{\mathbf{G}}_{2\times 2} = \bar{\mathbf{G}}/\Omega^2$, $\underline{\mathbf{K}}(\tau)_{2\times 2} = \left[\bar{\mathbf{K}}(\tau) - \bar{\mathbf{K}}_s\right]/\Omega^2$, $\mathbf{A}$ and $\mathbf{B}$ are the system matrices, $\mathbf{q} = [\bar{X}\bar{X}']^{\mathrm{T}}$ is the state vector of the rotor. $\mathbf{u} = [i_x i_y]^{\mathrm{T}}$ is the control current vector. $\mathbf{f}_e$ is the external force vector which includes the rotor imbalance and the gravity force. $\mathbf{I}$ is the unit matrix $\bar{X} = \{XY\}^{\mathrm{T}}$.

2.6. Optimal control

Generally, any effects of a crack in the rotor on the controller of the AMB are not taken into account at the initial design stage of the AMB controller. The AMB controller is designed only for the uncracked rotor system. In this case, $\bar{\mathbf{K}}(\tau)$ in Eq. (8) is a time invariant matrix and equals the stiffness of the uncracked rotor, i.e., $\bar{\mathbf{K}}(\tau) = diag(1)$.

Consider the quadratic performance index given by

$$\mathbf{J} = \int_0^\infty (\mathbf{q}^{\mathrm{T}}\mathbf{Q}\mathbf{q} + \mathbf{u}^{\mathrm{T}}\mathbf{R}\mathbf{u})\,\mathrm{d}t, \tag{11}$$

where $\mathbf{Q}$ and $\mathbf{R}$ are the positive semi-definite and positive definite weighting symmetric matrices for the state vector and the control current vector, respectively, then the solution to minimization of $\mathbf{J}$ is the optimal control law given by

$$\mathbf{u} = -\mathbf{R}^{-1}\mathbf{B}^{\mathrm{T}}\mathbf{P}\mathbf{q}, \tag{12}$$

where $\mathbf{P}$ is the solution of the following steady state algebraic Riccati matrix equation

$$\mathbf{P}\mathbf{A} + \mathbf{A}^{\mathrm{T}}\mathbf{P} - \mathbf{P}\mathbf{B}\mathbf{R}^{-1}\mathbf{B}^{\mathrm{T}}\mathbf{P} + \mathbf{Q} = \mathbf{0}. \tag{13}$$

If the system $[\mathbf{A}, \mathbf{B}]$ is controllable and $[\mathbf{A}, \mathbf{D}]$ is completely observable, where $\mathbf{D}$ is any matrix such that $\mathbf{D}\mathbf{D}^{\mathrm{T}} = \mathbf{Q}$, the positive definite solution matrix $\mathbf{P}$ always exists and the controlled system is asymptotically stable and the performance index can be reached. As a result, the optimal control force vector $\mathbf{u}_{opt}$, can be written using the feedback gain matrices as

$$\mathbf{u}_{opt} = -\mathbf{R}^{-1}\mathbf{B}^{\mathrm{T}}\mathbf{P}\mathbf{q} = -[\mathbf{K}_{opt}\mathbf{C}_{opt}]\mathbf{q} = -\{\mathbf{K}_{opt}\bar{X} + \mathbf{C}_{opt}\dot{\bar{X}}\}, \tag{14}$$

where $[\mathbf{K}_{opt}\mathbf{C}_{opt}] = \mathbf{R}^{-1}\mathbf{B}^{\mathrm{T}}\mathbf{P}$, $\mathbf{K}_{opt}$ and $\mathbf{C}_{opt}$ are optimal feedback stiffness and damping gain matrices.

Finally, the equations of motion of the cracked rotor with the AMB can be written in the general form

$$\underline{\mathbf{M}}\bar{X}'' + [\underline{\mathbf{C}} + \underline{\mathbf{G}}\mathbf{C}_{opt}]\bar{X}' + [\underline{\mathbf{K}}(\tau) + \bar{\mathbf{G}}\mathbf{K}_{opt}]\bar{X} = \frac{1}{\Omega^2}\begin{Bmatrix} 1 \\ 0 \end{Bmatrix} + U\begin{Bmatrix} \cos(\tau+\beta) \\ \sin(\tau+\beta) \end{Bmatrix}. \tag{15}$$

Since the equation of motion of the cracked rotor with the AMB is a non-linear system with a periodic stiffness coefficient, an exact solution is not possible. Numerical methods must be used to get the solutions in order to analyze the imbalance responses of the cracked rotor system. In this paper, the fourth order Runge–Kutta method with a constant time step size was used; the time step chosen was so small that the steady state responses of the rotor system were the same, even if the time step size was further decreased.

Since the orbits of the cracked rotor system with the AMB or without the AMB are non-synchronous at some regions of rotating speeds, the vibrations in the x or y direction are, respectively, the average values of the rotor motion orbits in the x or y direction in this paper.

3. Floquet stability theory

Since either the cracked rotor system without the AMB or with the AMB is linear periodic time varying, the Floquet theory may be used in order to analyze the stability of such periodic coefficient systems. From Eq. (15), one obtains the perturbation equations of motion of the cracked system with the AMB as

$$\underline{\mathbf{M}}\Delta\bar{X}'' + [\underline{\mathbf{C}} + \underline{\mathbf{G}}\mathbf{C}_{opt}]\,\Delta\bar{X}' + [\underline{\mathbf{K}}(\tau) + \underline{\mathbf{G}}\mathbf{K}_{opt}]\,\Delta\bar{X} = 0. \tag{16}$$

So, the first order state perturbation equations of motion of the system can be obtained and written in the matrix form as

$$\delta\mathbf{q}' = \begin{bmatrix} \mathbf{0} & \mathbf{I} \\ -\underline{\mathbf{M}}^{-1}(\underline{\mathbf{K}}(\tau) + \underline{\mathbf{G}}\mathbf{K}_{opt}) & -\underline{\mathbf{M}}^{-1}(\underline{\mathbf{C}} + \underline{\mathbf{G}}\mathbf{C}_{opt}) \end{bmatrix}\delta\mathbf{q} = [\mathbf{H}(\tau)]\delta\mathbf{q}, \tag{17}$$

where $\delta\mathbf{q} = \{\Delta\bar{X}\,\Delta\bar{Y}\,\Delta\bar{X}'\,\Delta\bar{Y}'\}^{\mathrm{T}}$ and $\mathbf{H}(\tau) = \mathbf{H}(\tau + 2\pi)$ is a periodic coefficient matrix with period 2π.

From the Floquet stability theory, one has to calculate the transition matrix of the periodic time-varying system over a period $T = 2\pi$, $\mathbf{\Gamma}(\tau)$. This matrix will tell one how the state vector $\mathbf{q}(\tau)$ of the system has changed after one period T. The relationship of the state of the system after one period T with the initial state can be expressed as

$$\mathbf{q}(\tau + T) = \mathbf{\Gamma}(\tau)\mathbf{q}(\tau). \tag{18}$$

It is clear that if the transition matrix $\mathbf{\Gamma}(\tau)$ is known, the stability of the system can be determined from the eigenvalue of the equation

$$|\mathbf{\Gamma}(\tau) - \mu\mathbf{I}| = 0, \tag{19}$$

where μ is the Floquet multiplier and gives the conditions of stability. If the modulus of every eigenvalue $|\mu|$ is less than unity, the system is stable, otherwise the system is unstable.

Table 1
Specifications of rotor and AMB

$m = 5.0$	(kg)
$k_0 = 10^6$	(N/m)
$e_\mu = 0.5$	(mm)
$i_{0x} = i_{0y} = 0.8$	(A)
$k_{sx} = k_{sy} = 1000$	(N/mm)
$k_{ix} = k_{iy} = -200$	(N/A)

Although the stability of the periodic time-varying system can be determined from the transition matrix of the system, unfortunately, there is no general analytical method for calculating the transition matrix $\mathbf{\Gamma}(\tau)$ for multi-variable systems. Therefore, the problem for determining the system stability becomes the numerical calculation of the transition matrix $\mathbf{\Gamma}(\tau)$.

In order to obtain the $\mathbf{\Gamma}(\tau)$, the period T is divided into a number n of intervals of length $h = T/n$, in such a way that it is possible to consider that $\mathbf{H}(\tau_i)$ is a constant on each small interval $[ih(i+1)h]$. The elementary transition matrices $\mathbf{\Gamma}(\tau_i)$ over the different intervals are calculated by using formula given by Guilhen et al. [11] as

$$\mathbf{\Gamma}(i) = \mathbf{I} + (h/2)\,(\mathbf{H}(\tau_i) + \mathbf{H}(\tau_{i+1}))\big(\mathbf{I} + (h/2)\,\mathbf{H}(\tau_{i+1})\big). \tag{20}$$

The finial transition matrix over one period is given by

$$\mathbf{\Gamma}(T) = \mathbf{\Gamma}(n-1)\mathbf{\Gamma}(n-2), \ldots, \mathbf{\Gamma}(i-1)\mathbf{\Gamma}(i), \ldots, \mathbf{\Gamma}(1)\mathbf{\Gamma}(0). \tag{21}$$

After obtaining numerically the transition matrix over a period T, $\mathbf{\Gamma}(T)$, the stability of the cracked rotor with or without the AMB can be analyzed by the Floquet method.

4. Numerical results and analyses

The specifications of the rotor and the AMB are listed in Table 1.

4.1. The dynamics of the cracked rotor without the AMBs

Many papers exist describing the dynamic behaviour of cracked rotors [1–7]. Before discussing the stability and imbalance response of a cracked rotors with the AMBs, the main results of dynamic behaviour of cracked rotor systems without the AMBs, is briefly summarized.

Fig. 2. Dynamic behaviour of the cracked rotor: (a) effect of the crack depth on rotor vibration ($\zeta = 0.05, \beta = 0.0, k_\eta = 1, U = 0.05$); (b) effect of crack depth on $1\times$, $2\times$ and $3\times$ super-harmonic frequency vibration amplitudes ($\zeta = 0.05, \beta = 0.0, k_\eta = 1, U = 0.05$); (c) effect of the damping ratio on rotor vibration ($\beta = 0.0, k_\zeta = 0.9, k_\eta = 1, U = 0.05$); (d) effect of the imbalance phase angle on rotor vibration ($\zeta = 0.05, k_\zeta = 0.9, k_\eta = 1, U = 0.05$); (e) effect of the imbalance parameter on rotor vibration ($\zeta = 0.05, k_\zeta = 0.9, k_\eta = 1, \beta = 0.0$); (f) effect of the damping ratio on unstable regions ($k_\zeta = 0.8, k_\eta = 1, \beta = 0.0$); and (g) the minimum damping ratio for suppressing instable regions ($k_\eta = 1, \beta = 0.0$).

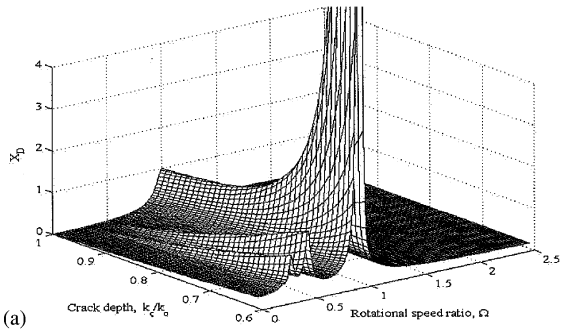
X_D
Crack depth, k_ζ/k_o
Rotational speed ratio, Ω

(a)

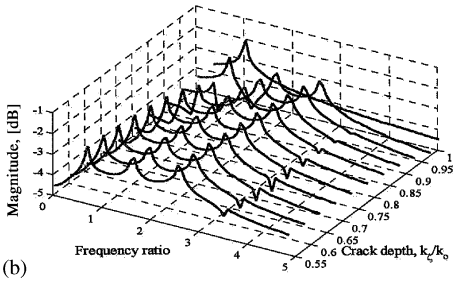
Magnitude, [dB]
Frequency ratio
Crack depth, k_ζ/k_o

(b)

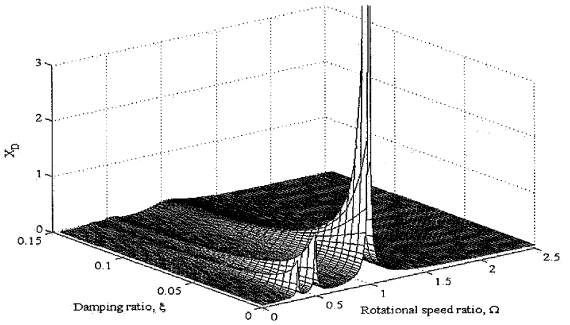
X_D
Damping ratio, ξ
Rotational speed ratio, Ω

(c)

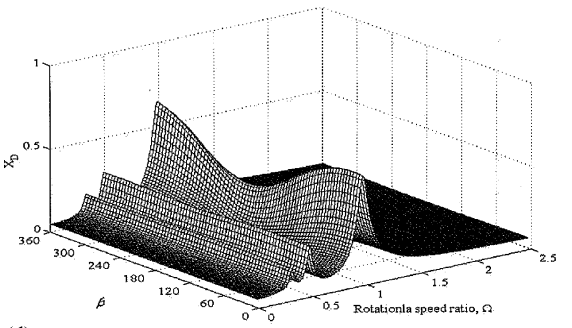
X_D
β
Rotationla speed ratio, Ω

(d)

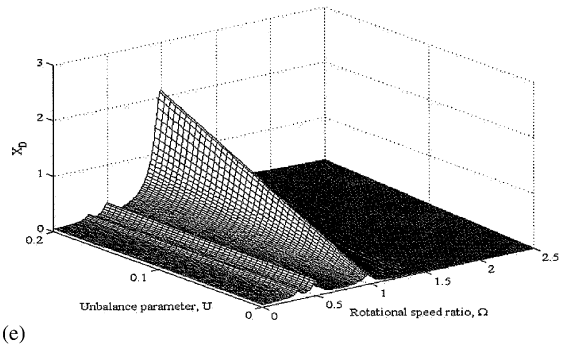
X_D
Unbalance parameter, U
Rotational speed ratio, Ω

(e)

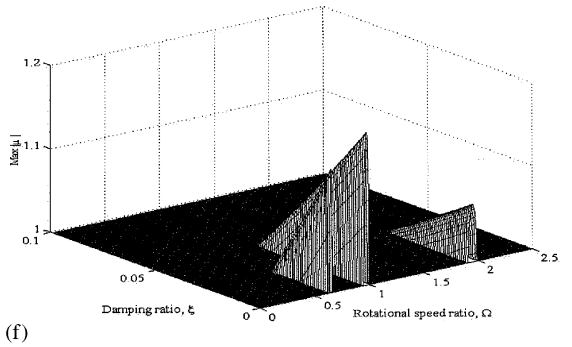
Max|μ|
Damping ratio, ξ
Rotational speed ratio, Ω

(f)

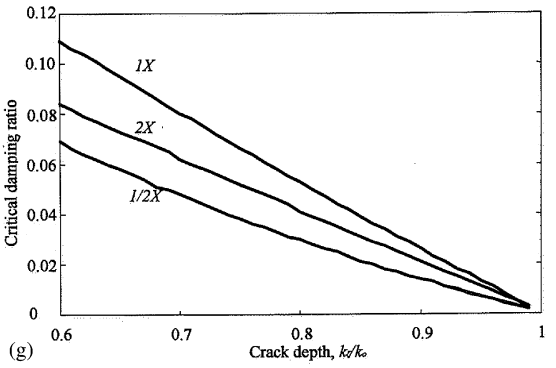
1X
2X
1/2X
Critical damping ratio
Crack depth, k_ζ/k_o

(g)

(1) The interaction of the crack breathing action, gravity and rotor imbalance results in many n-per-revolution (nx) super-harmonic frequency components in the vibration signals or additional sub-resonances at rotating speeds of nominally $1/n$ times the synchronous critical speed in the imbalance response curves as shown in Fig. 2a and b. In particular, the $2\times$ and $3\times$ super-harmonic frequency components or $\frac{1}{2}$ and $\frac{1}{3}$ sub-critical resonances are significant. The synchronous critical speeds are defined as those rotational speeds of the uncracked rotor system, which basically correspond to the natural whirl frequencies of the uncracked rotor system. The former is produced by the periodic time-variant system and the reason for the latter is that one of the super-harmonics resonates at the sub-critical speed. In some instances, the super-harmonic frequency can be more prominent than the rotational frequency. Note that the $1/n$th order sub-critical resonance is caused by the nth order super-hamonic frequency component.With the increase of the crack depth, the $2\times$ and $3\times$ amplitudes or the $\frac{1}{2}$ and $\frac{1}{3}$ sub-critical resonant peaks increase obviously, as shown in Fig. 2a. The main resonant speed of the cracked rotor decreases with the increase of the crack depth, but its change is small and it is impossible to use this change to detect the existence of a crack.

(2) The motion of the cracked rotor is complicated due to existence of the $1\times$, $2\times$, $3\times$, etc. frequencies of the rotational speed in the vibration signals, but the period of these motions is equal to the period of the exciting force, i.e., rotor rotating motion.

(3) With any increase of damping, the resonant amplitudes in both the main critical speed and the sub-critical speeds are gradually suppressed as shown in Fig. 2c.

(4) For a given crack depth, the $1\times$ revolution vibration amplitude is associated with the rotor imbalance and the position of the imbalance relative to the crack direction as shown in Fig. 2d. It is a maximum when the imbalance is in phase with the crack, and minimum when out of phase with the crack. With the increase of the rotor imbalance, only the $1\times$ amplitude increases, the other $2\times$, $3\times\ldots$ amplitudes do not greatly change at all since the sub-critical resonances are caused by gravity force as shown in Fig. 2d.

(5) It is clear the vibration amplitudes in the sub-critical resonances depend on the cracked depth and the rotor damping. If the damping ratio remains virtually constant during operation of machines, the $2\times$ and $3\times$ amplitude changes in the run-up or run-down operation can be used as indexes for the detection of any cracks. When the rotor is running at a constant speed for a long period, the $2\times$ and $3\times$ amplitudes increase with the crack growth. This information can be used to detect the cracks as used by Imam et al. [9].

(6) For a rotor system with slight damping, the existence of a crack produces more unstable regions except in the vicinity of the main critical speed as shown in Fig. 2e. The unstable regions near the rotational speeds at the $\frac{1}{2}$, 1, 2 of the critical speed will expand with an increase of crack depth. Besides the three larger unstable regions, other regions exist at lower speeds, but these regions are very narrow. If the damping of the rotor system is relatively high, the unstable regions will disappear. The smallest damping required to suppress the instability in the different regions of rotational speeds are shown in Fig. 2f. It is shown that a rotor system running in bearings with high damping are normally sufficient to prevent the occurrence of these instability regions when a crack appears.

4.2. Effect of the crack on the control system

Selection of the weighting matrices **Q** and **R** is arbitrary except that the requirement of positive definiteness must be satisfied. There are different selection methods of weighting matrices **Q** and **R**. In this paper, the **Q** and **R** matrices are chosen to be diagonal, i.e.,

$$\mathbf{Q} = diag(g), \quad \mathbf{R} = diag(r). \tag{22}$$

The optimal control based on the uncracked rotor system only can make the uncracked rotor system asymptotically stable and minimize the performance index. The system stability does not depend on the **Q** and **R**, but the performance index. However, the most important problem is whether the initial control system in which the effect of any crack is ignored is stable or not, when cracks appear. The effect of the crack on the stability of the initial control system is shown in Fig. 3 for different **Q**'s when $\mathbf{R} = \mathbf{1}$. The corresponding imbalance response curves of the rotor–AMBs system are shown in Fig. 4. It is shown that the optimal control cannot always guarantee that the cracked rotor–AMB system is stable, the stability of the cracked rotor–AMB system will depend on the values of **R** and **Q**. Instability will occur when the vibration of the rotor system is not fully controlled. The larger the vibration of the cracked rotor–AMB system, or the smaller the q/r is, the higher the possibility of an instability occurring. Fortunately, the general rule for the selection of **R** and **Q** is to make the vibration of the rotor system as small as possible. Therefore, if the control system is effective for controlling the rotor vibration, the control system will be stable even if the crack appears.

However, as there exists a potential instability problem in the cracked rotor–AMB system with the optimal controller of the uncracked rotor, the controller design should be based on the periodic time-varying cracked rotor system. In this way, the optimal control can make the cracked rotor stable and minimize the rotor vibration. The control problem of periodic time-varying

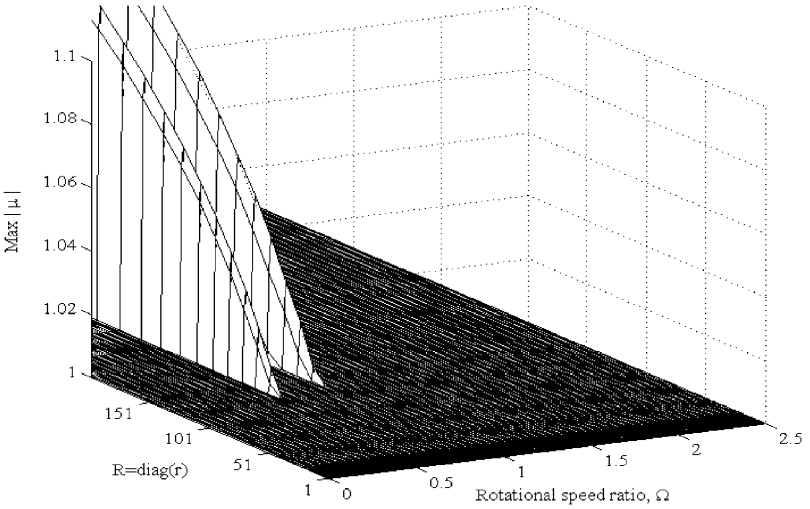

Fig. 3. Stability of the cracked rotor–AMB system with optimal control gains ($q = 1, \zeta = 0.05$, $k_\zeta = 0.9$, $k_\eta = 1$, $\beta = 0.0$).

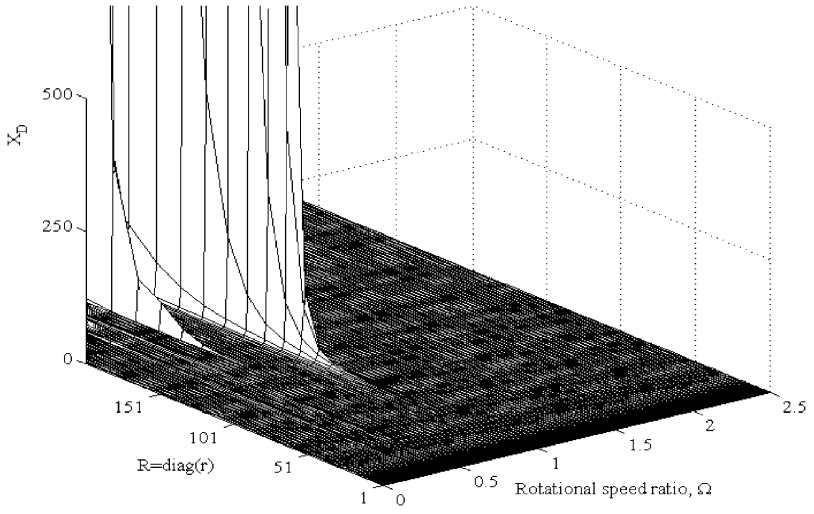

Fig. 4. Imbalance response of the cracked rotor–AMB system with same optimal control gains as in Fig. 3.

systems is very complicated and has been studied by Anton and Ulbrich [12], Sinha and Joseph [13].

4.3. Imbalance response of the rotor–AMB system

The imbalance responses of the cracked rotor–AMB system with a given crack depth for different **Q**'s and **R**'s are shown in Fig. 5. Where the dashed line for the active cracked rotor with $\mathbf{Q} = \mathbf{R} = 1$, the lines below the dashed line are with $q/r = 5$, 10, 20, 50 and 100, the lines above the dashed line are with $q/r = \frac{1}{5}$, $\frac{1}{10}$, $\frac{1}{20}$, $\frac{1}{50}$ and $\frac{1}{100}$, respectively. It is shown that whether the main and sub-critical resonances appear or not in the cracked rotor–AMB system mainly depends on the weighting matrices **Q** and **R**.

When **Q** is small and **R** is large, or q/r is small, i.e., more attention is paid to the controller and less to the rotor vibration, the effect of the controller or the AMB on the rotor system is very weak, the sub-resonances and the main resonance will appear and locate at the speeds just lower than the cracked rotor system without the AMB as shown in Fig. 6(a) and (b). The variations of the rotor orbits and super-harmonic frequency components with the crack depth at $\Omega = 0.3$ and 1.5 are shown in Fig. 6(c)–(f). The arrow in the figures is the direction of increasing crack depth. It is shown that if **Q** and **R** are fixed, the super-harmonic frequency components of $2\times$ and $3\times$ revolutions increase with crack depth. The orbits are also changed with crack depth, especially in the sub-critical speed region. In this case, it is still possible to use the traditional method where the $2\times$ and $3\times$ super-harmonic frequency components are used as indices to diagnose the crack in the AMB–rotor system. The effect of the rotor imbalance parameter, damping and imbalance phase angle on the dynamic behaviour of the cracked rotor–AMB system are shown in Fig. 7. It is shown that in this case, the dynamic behaviour of the cracked rotor–AMB system is very similar to that of the cracked rotor systems without the AMB.

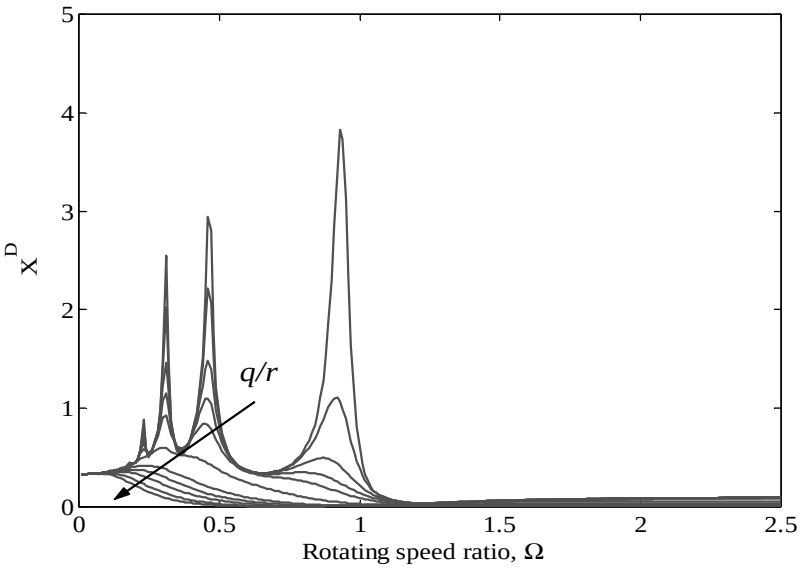

Fig. 5. Effect of **Q** and **R** on imbalance responses of the rotor–AMB system for a given crack depth ($\xi = 0.05, k_\zeta = 0.9$, $k_\eta = 1, \beta = 0.0$).

When **Q** is large and **R** is small or q/r is large, i.e., more attention is paid to the rotor vibration and less to the controller and assume that the AMB can produce large enough control forces, the vibration of the rotor system is basically or completely controlled and the main resonance does not appear at all. This is the desired result of using the AMB. If the q/r is not too large, for example, $q/r = 10$ in Fig. 8, there is a peak in the imbalance response curves with large crack depths, but the peak positions are neither at $\frac{1}{2}$ nor $\frac{1}{3}$ of the critical speed. If the q/r is very large, for example, $q/r = 100$ in Fig. 8, there is not a peak in the imbalance response curves even if the crack depth is very large. The rotor orbits and corresponding $2\times$ and $3\times$ revolution super-harmonic frequency components with crack depth at $\Omega = 0.3$ and 1.5 are shown in Fig. 7(c)–(f) and Fig. 8(c)–(f). In these cases with small rotor vibration, the orbits in the sub-critical speed region change with an increase in the crack depth and there are $2\times$ and $3\times$ revolution super-harmonic frequency components in the rotor vibrations, but in the super-critical speed region, the orbits show virtually no change and there are no $2\times$ and $3\times$ revolution super-harmonic frequency components. Therefore, it is impossible to use the $2\times$ and $3\times$ revolution super-harmonic frequency components in the super-critical speed region as proposed by Imam et al. [9] to detect the crack.

Therefore, for the rotor–AMB system with fixed **Q** and **R** in the optimal controller, only the $2\times$ and $3\times$ super-harmonic frequency components in the sub-critical speed region can be used as indications of the existence of a crack in the active cracked rotor system. If **Q** and **R** in the controller are varied as the crack depth grows or the rotor vibrations increase, then the $2\times$ and $3\times$ super-harmonic frequency components in the sub-critical speed region will not always increase with an increase in the crack depth, the effect of the crack on the vibration characteristics of the rotor–AMBs system will be very complex. However, since a controlled exciting force can be

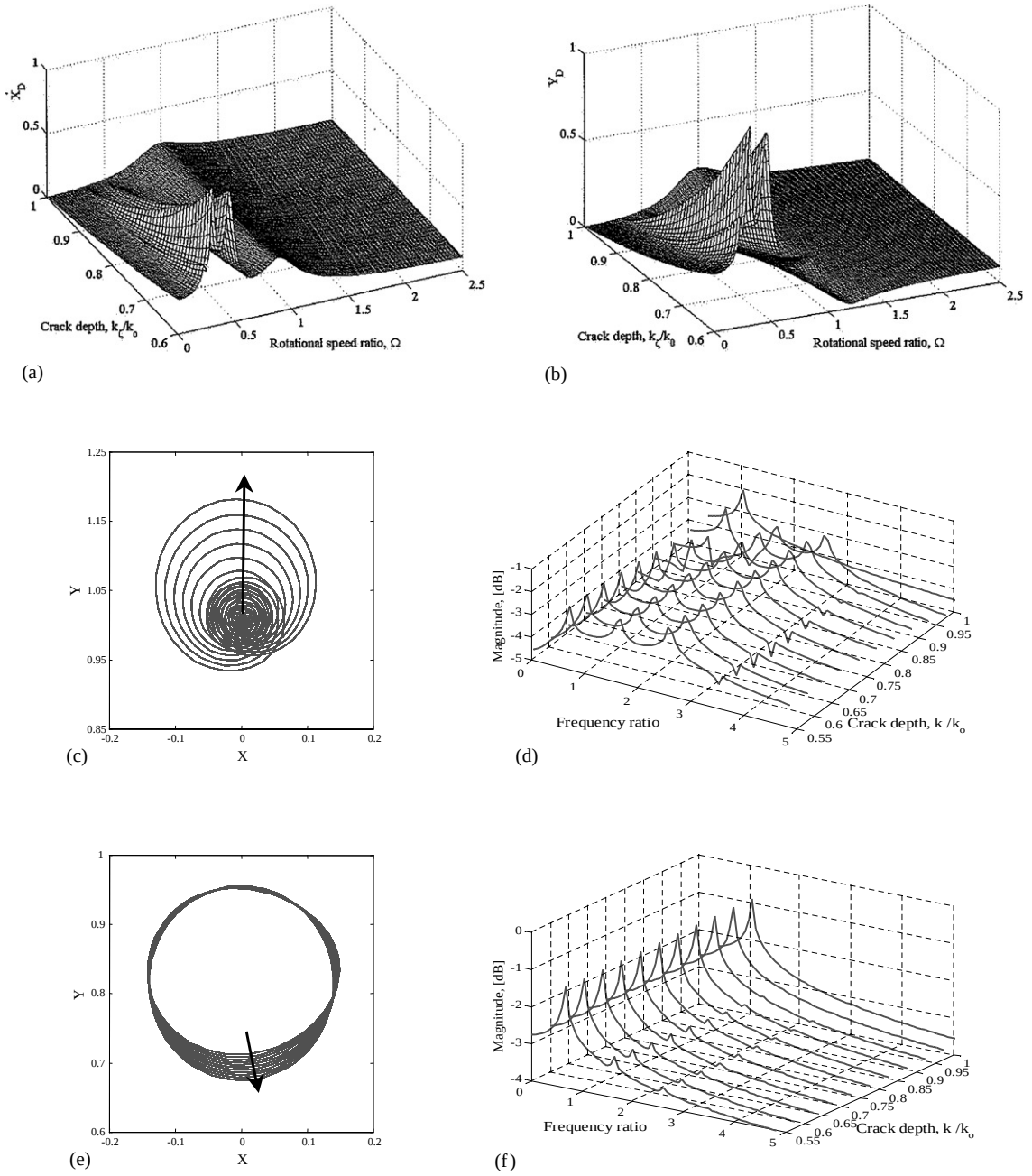

Fig. 6. The effect of the crack depth on the dynamics of the cracked rotor–AMB system ($q = 1$,$r = 10$, $U = 0.1$, $\xi = 0.01$, $k_\eta = 1, \beta = 0.0$): (a) and (b) for variation of imbalance response of the cracked rotor–AMB system with crack depth; (c) and (d) for rotor orbits and super-harmonic components with crack depth at $\Omega = 0.3$; (e) and (f) for rotor orbits and super-harmonic components with crack depth at $\Omega = 1.5$.

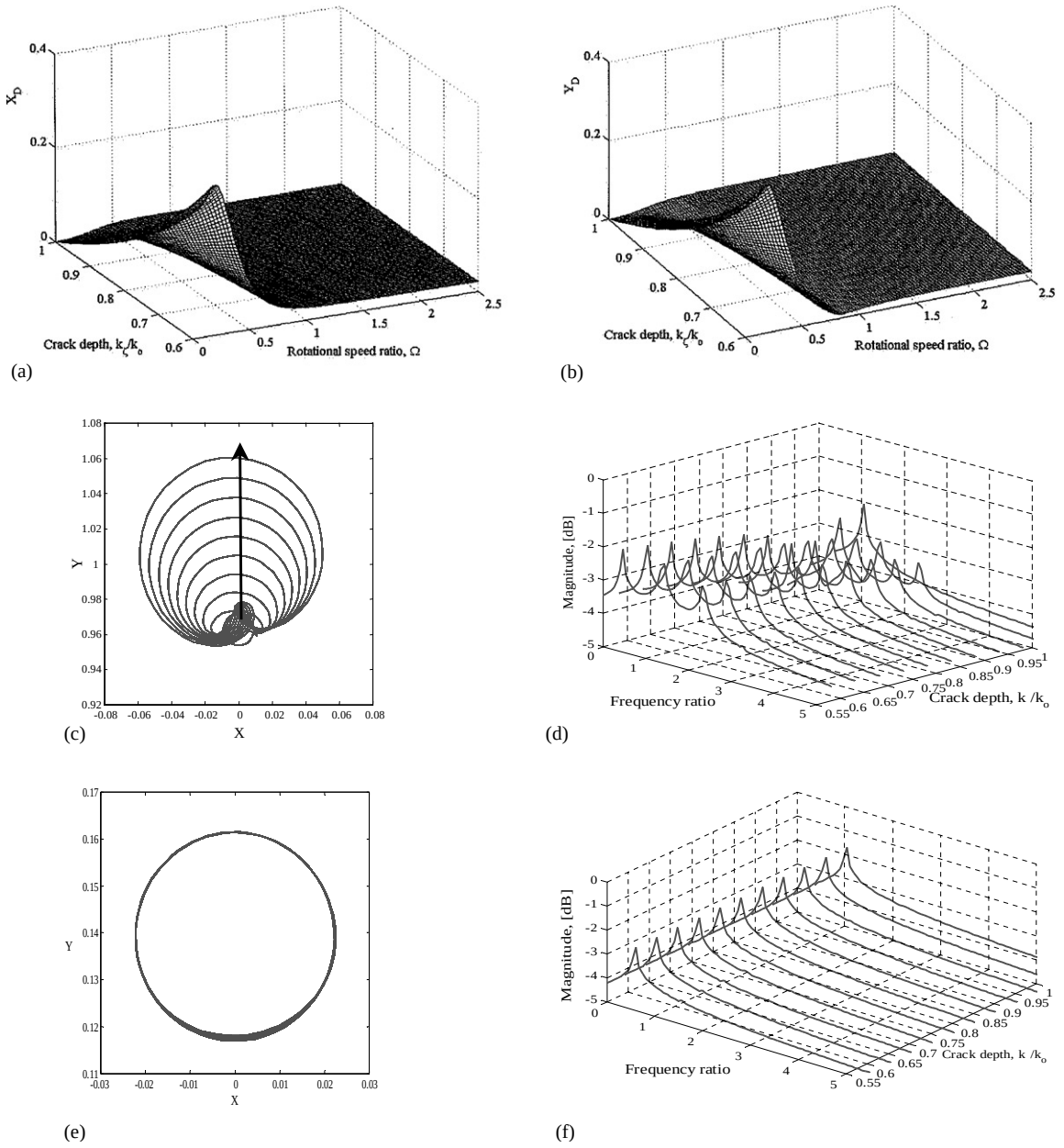

Fig. 7. The effect of the crack depth on the dynamics of the cracked rotor–AMB system ($q = 10, r = 1, U = 0.1, \xi = 0.01, k_\eta = 1, \beta = 0.0$): (a) and (b) for variation of imbalance response of the active cracked rotor–AMB system with crack depth; (c) and (d) for rotor orbits and super-harmonic components with crack depth at $\Omega = 0.3$; (e) and (f) for rotor orbits and super-harmonic components with crack depth at $\Omega = 1.5$.

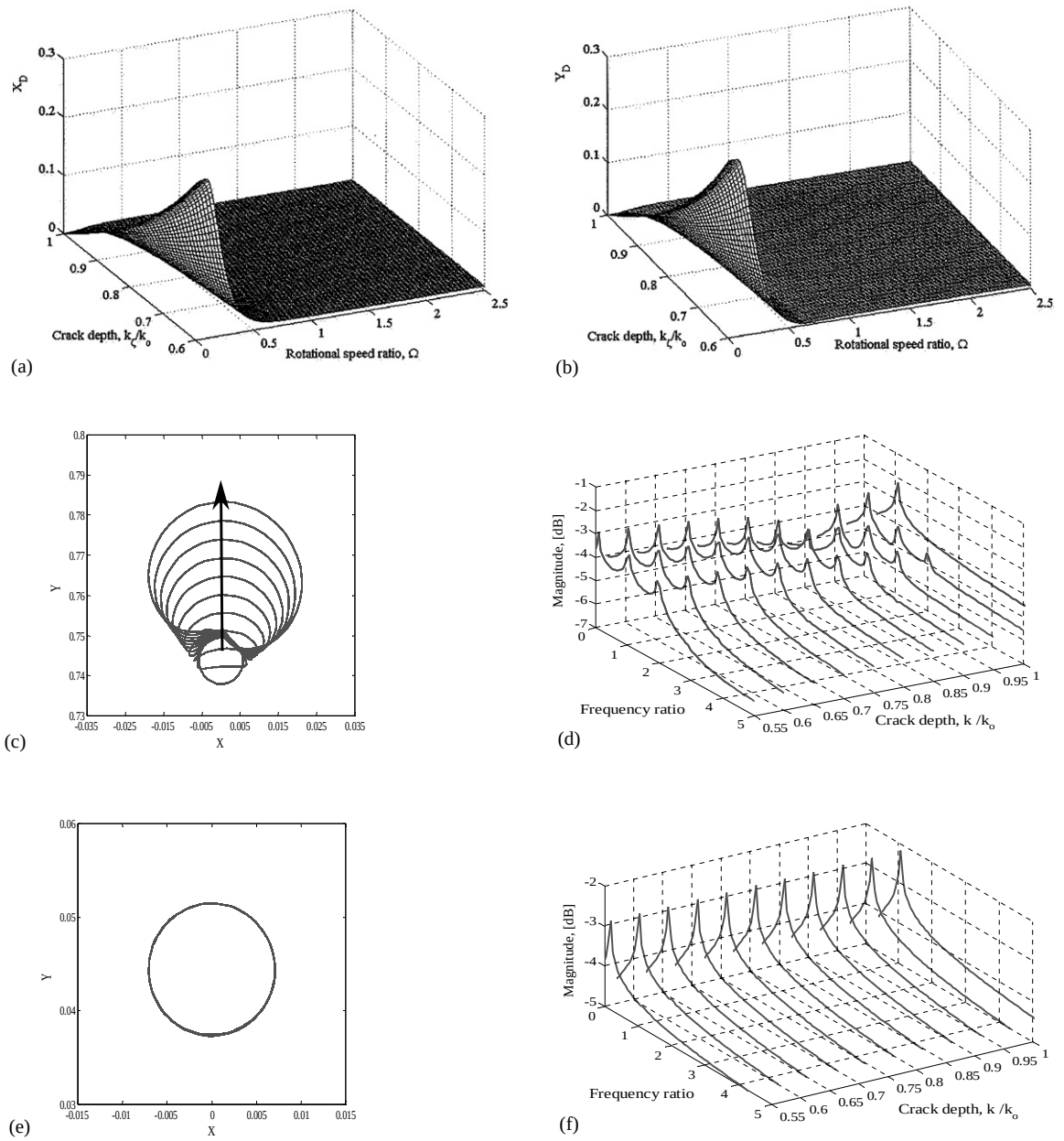

Fig. 8. The effect of the crack depth on the dynamics of the cracked rotor–AMB system ($q = 100, r = 1, U = 0.1, \xi = 0.01, k_\eta = 1, \beta = 0.0$): (a) and (b) for variation of imbalance response of the cracked rotor–AMB system with crack depth; (c) and (d) for rotor orbits and super-harmonic components with crack depth at $\Omega = 0.3$; (e) and (f) for rotor orbits and super-harmonic components with crack depth at $\Omega = 1.5$.

applied to the rotating rotor system by means of the AMBs when the rotor is running, it is possible to use this benefit of the AMB to study the change of the dynamic characteristics of active cracked rotor systems to diagnose the crack in active rotor systems. This work is still in progress, the result will be reported later.

5. Conclusions

The effect of cracks on the rotor system should be considered in designing the AMB controller, otherwise unstable motion in some regions of the rotational speed range is possible if cracks occur.

The dynamic characteristics of a cracked rotor with AMB supports are obviously more complex than that of the traditional cracked rotor system. Only the $2\times$ and $3\times$ revolution super-harmonic components in the sub-critical speed region can be used to detect a crack in the rotor–AMB system. It is impossible to use the traditional method with the $2\times$ and $3\times$ revolution super-harmonic frequency components in the super-critical speed region to detect the crack.

For more complex control algorithms, for example, H_α, robust adaptive control, variable structure control, etc., the $2\times$ and $3\times$ super-harmonic frequency components in the sub-critical speed region do not always increase with the increase of the crack depth, hence it may be very difficult to diagnose a crack in the AMB–rotor system and alternative diagnosis methods of the crack should be studied.

Acknowledgements

The work is supported by the EC BRITE/EURAM program under BRPR-CT97-0544 IMPACT project.

Appendix A. Nomenclature

A	flux cross-sectional area of the air-gap
$\mathbf{A}$, $\mathbf{B}$	system matrices
c	external damping coefficient at the mid-plane disc
$\mathbf{C}_{opt}$	optimum feedback damping gain matrix
$\underline{\mathbf{C}}$	damping matrix, $\underline{\mathbf{C}} = diag(2\xi/\Omega)$
$\mathbf{D}$	system matrix, $\mathbf{D}\mathbf{D}^{\mathrm{T}} = \mathbf{Q}$
e_u	imbalance eccentricity of the disc
$\mathbf{f}_e$	external force vector
F_x, F_y	feedback control forces in the x and y directions in the Cartesian co-ordinate system
$\mathbf{g}$	acceleration due to gravity
$\mathbf{G}$	current stiffness matrix of the ABM
$\bar{\mathbf{G}}$	non-dimensional current stiffness matrix of the ABM

$\underline{\mathbf{G}}$	$= \bar{\mathbf{G}}/\Omega^2$
$\boldsymbol{H}(\tau)$	periodic coefficient matrix with period 2π
i_x, i_y	control currents of the AMB in the x and y directions
i_{0x}, i_{0y}	bias currents of the AMB in the x and y directions
$\boldsymbol{I}$	unit matrix
$\boldsymbol{J}$	performance index
k_{ix}, k_{iy}	current stiffness elements of the AMB in the x and y directions
$k_m, \Delta k$	non-dimensional stiffness and average stiffness variation defined in paper
$k_{m\zeta}, k_{m\eta}$	average stiffnesses of the cracked rotor in the minimum and maximum stiffness directions (i.e., ζ and η)
k_0	stiffness of the uncracked rotor in the disc position
k_{sx}, k_{sy}	displacement stiffness elements of the AMB in the x and y directions
k_ζ, k_η	stiffnesses of the cracked rotor in the ξ and η directions in the rotating co-ordinate system
$\bar{k}_\zeta, \bar{k}_\eta$	non-dimensional stiffnesses of the cracked rotor in the ξ and η directions
$\Delta k_\zeta, \Delta k_\eta$	stiffness variations of the cracked rotor in the ξ and η directions
$\Delta k_{m\zeta}, \Delta k_{m\eta}$	stiffness variations of the cracked rotor in the ξ and η directions
$\mathbf{K}(t)$	stiffness matrix of the cracked rotor
$\bar{\mathbf{K}}(\tau)$	non-dimensional stiffness matrix of the cracked rotor in the stationary co-ordinate system
$\mathbf{K}_{opt}$	optimum feedback stiffness gain matrix
$\mathbf{K}_s$	displacement stiffness matrix of the AMB
$\bar{\mathbf{K}}_S$	non-dimensional displacement stiffness matrix
m	equivalent mass in the disc position
$\underline{\mathbf{M}}$	mass matrix
N	number of the windings of the coil
$\mathbf{P}$	solution of the optimum feedback control
$\mathbf{q}$	state vector of the rotor system
$\Delta\mathbf{q}$	First order state perturbation vector
$\mathbf{Q}$	positive semi-definite weighting matrix
$\mathbf{R}$	positive definite weighting matrix
s	nominal air-gap of the AMB
t	time
T	period of the exciting force
$\mathbf{u}$	control current vector
$\bar{\mathbf{U}}$	rotor imbalance parameter, $\bar{\mathbf{U}} = e_\mu/\delta_{st}$
$\mathbf{u}_{opt}$	optimum control force vector
x, y	Cartesian co-ordinates
X, Y	$X = x/\delta_{st},\ Y = y/\delta_{st}$
$\Delta X,\ \Delta Y$	$\Delta X = \Delta x/\delta_{st},\ \Delta Y = \Delta y/\delta_{st}$
β	relative phase angle of disc imbalance force vector with respect to the minimum stiffness direction of the crack
μ	Floquet multiplier
μ_0	air permeability

τ	non-dimensional time, $\tau = \omega t$
ω	rotational speed
ω_{cr}	first pin–pin critical speed of the uncracked rotor mounted rigidly, $\omega_{cr} = \sqrt{k_0/m}$.
δ_{st}	deformation of the shaft due to rotor weight
Ω	rotational speed ratio, $\Omega = \omega/\omega_{cr}$
ξ	linear air damping ratio, $\xi = c/2\,m\omega_{cr}$
$\Gamma(\tau)$	transition matrix
$'$	$\mathrm{d}/\mathrm{d}\tau$
$\cdot$	$\mathrm{d}/\mathrm{d}t$

References

[1] J. Wauer, On the dynamics of cracked rotors: a literature survey, Applied Mechanics Reviews 43 (1990) 13–17.

[2] R. Gasch, Dynamic behaviour of a simple rotor with a cross-sectional crack, Proceedings of the Vibrations in Rotating Machinery, Institution of Mechanical Engineering, Cambridge, UK, 1976, pp. 123–128.

[3] R. Gasch, A survey of the dynamics behaviour of a simple rotating shaft with a transverse crack, Journal of Sound and Vibration 160 (1993) 313–332.

[4] A. Maszynska, Shaft crack detection, Proceedings of the Seventh Machinery Dynamic Seminar, Edmonton, Canada, 1982.

[5] B. Grabowski, Journal of Mechanical Design 102 (1980) 140–146.

[6] W. Mayes, W.G.R. Davies, Analysis of the response of a multi-rotor-bearing system containing a transverse crack in a rotor, Journal of Vibration Acoustics Stress and Reliability in Design 106 (1984) 139–145.

[7] H.D. Nelson, C. Nataraj, The dynamics of a rotor system with a cracked shaft, Journal of Vibration Acoustics Stress and Reliability in Design 108 (1986) 189–196.

[8] C.S. Zhu, D.A. Robb, D.J. Ewins, The dynamics of a cracked rotor with active feedback control system, Proceedings of the Eighth International Symposium of Magnetic Bearings, ETH, Zurich, 2000, pp. 323–330.

[9] I. Imam, S.H. Azzaro, R.J. Banket, J. Scheibel, Development of an on-line rotor crack detection and monitoring system, ASME Journal of Vibration, Acoustics, Stress, and Reliability in Design 111 (1989) 241–250.

[10] G. Schweitzer, H. Bleuler, A. Traxler, Active magnetic bearings, basic, properties and application of active magnetic bearings, Vdf Hochschulverlag AG an der ETH, Zurich, 1994.

[11] M. Guilhen, P. Berthier, G. Ferraris, M. Lalanne, Instability and unbalance response of asymmetric rotor-bearing systems, ASME Journal of Vibration, Acoustics, Stress, and Reliability in Design 110 (1988) 288–294.

[12] E. Anton, H. Ulbrich, Active control of vibrations in the case of asymmetrical high-speed rotors by using magnetic bearings, Journal of Vibration Acoustics Stress and Reliability in Design 107 (1989) 410–415.

[13] S.C. Sinha, P. Joseph, Control of general dynamic systems with periodically varying parameters via Liapunov–Floquet transformation, Journal of Dynamic System Measurement and Control 116 (1994) 650–658.